Geophysical Research Letters

RESEARCH LETTER
10.1029/2019GL083593

Observational Evidence for Throat Aurora Being Associated With Magnetopause Reconnection

De-Sheng Han[1], Tong Xu[2], Yaqi Jin[3], K. Oksavik[4,5], Xiang-Cai Chen[6], Jian-Jun Liu[6], Qinghe Zhang[7], Lisa Baddeley[4,5], and Katie Herlingshaw[4,5]

[1]State Key Laboratory of Marine Geology, School of Ocean and Earth Science, Tongji University, Shanghai, China, [2]National Key Laboratory of Electromagnetic Environment, China Research Institute of Radiowave Propagation, Qingdao, China, [3]Department of Physics, University of Oslo, Oslo, Norway, [4]Birkeland Centre for Space Science, Department of Physics and Technology, University of Bergen, Bergen, Norway, [5]The University Centre in Svalbard, Longyearbyen, Norway, [6]SOA Key Laboratory for Polar Science, Polar Research Institute of China, Shanghai, China, [7]Shandong Provincial Key Laboratory of Optical Astronomy and Solar-Terrestrial Environment, Institute of Space Sciences, Shandong University, Weihai, China

Key Points:
- An EISCAT radar experiment was designed to investigate the ionospheric characteristics of throat aurora
- Mesoscale twin flow cells, Joule heating effects, and ion upflows were associated with the throat aurora
- The observations support the idea that throat auroras are associated with magnetopause reconnection

Correspondence to:
D.-S. Han,
handesheng@tongji.edu.cn

Citation:
Han, D.-S., Xu, T., Jin, Y., Oksavik, K., Chen, X.-C., Liu, J.-J., et al. (2019). Observational evidence for throat aurora being associated with magnetopause reconnection. *Geophysical Research Letters*, *46*, 7113–7120. https://doi.org/10.1029/2019GL083593

Received 3 MAY 2019
Accepted 11 JUN 2019
Accepted article online 20 JUN 2019
Published online 1 JUL 2019

Abstract Throat auroras have been suggested to be related to indentations on the subsolar magnetopause. However, the indentation generation process and the resulting ionospheric responses have remained unknown. An EISCAT Svalbard Radar experiment was designed to run with all-sky cameras, which enabled us for the first time to observe the temporal and spatial evolution of flow reversals, Joule heating, and ion upflows associated with throat aurora. The high-resolution data enabled us to discriminate that the flow bursts and Joule heating were concurrent and co-located, but were always observed on the west side of the associated throat auroras, reflecting that the upward/downward field-aligned currents associated with throat aurora are always to the east/west, respectively. These results are consistent with the geometry of Southwood (1987) flux transfer event model and provide strong evidence for throat aurora being associated with magnetopause reconnection events. The results also support a conceptual model of the throat aurora.

1. Introduction

During a study on dayside diffuse aurora based on optical observations in the green line (557.7 nm), Han et al. (2015) noticed that, when a convection-aligned stripy diffuse aurora was contacting with the discrete aurora oval, a north-south aligned discrete auroral form was often observed. Because this particular auroral form was only observed around the ionospheric convection throat region, it was named "throat aurora" (Han et al., 2015). Later, based on careful examination, Han et al. (2017) pointed out that throat aurora should be the same phenomenon as the "crewcut" named by Rodriguez et al. (2012), although Rodriguez et al. (2012) found this auroral form in the red line (630.0 nm) observation and did not mention any relation between crewcut and diffuse aurora.

Based on the observational facts that throat auroras are caused by precipitation of magnetosheath particles, Han et al. (2016) suggested that throat auroras should correspond to localized magnetopause deformations. These deformations are supposed to be dented structures on the subsolar magnetopause. Later, Han et al. (2018) found one-to-one correspondences between throat auroras observed on the ground and magnetopause transients observed near the subsolar magnetopause, which have been suggested to be the direct evidence for throat auroras being the ionospheric signature of magnetopause indentations. In addition, it was found that the spatial scale of the magnetopause indentation can be as large as ~2.0 × 3.0 R_E (Earth radius) after mapping a throat aurora to the geomagnetic equatorial plane, and the occurrence rates are as high as ~50% and ~25% counted by day and by 10 min, respectively (Han et al., 2017). These observational results have indicated that the throat aurora is an important phenomenon for the dayside solar wind-magnetosphere-ionosphere coupling.

While considering the generation of throat auroras, Han et al. (2017) noticed that throat auroras were closely involved with diffuse aurora and their orientations were convection-aligned. This means that the occurrence of throat aurora is affected by factors inside the magnetosphere, because both diffuse aurora and convection are linked to magnetospheric internal phenomena. At the same time, Han et al. (2017) noticed that the

occurrence rate of throat aurora showed a clear dependence on the interplanetary magnetic field (IMF) cone angle (arccos[$|B_x|/B_{total}$)]), which suggested that some transient processes outside the magnetosphere, such as magnetosheath high-speed jets (Hao et al., 2016; Plaschke et al., 2018), might be a driver for throat auroras (Han et al., 2017). In order to explain why the generation of throat aurora depends on factors either inside or outside the magnetosphere, Han (2019) proposed a model and suggested that throat auroras should be caused by magnetopause reconnection, which can be affected by factors either inside or outside the magnetosphere. However, observational evidence for throat aurora being associated with magnetopause reconnection is very limited. One exception is Chen et al. (2017), who reported that the throat aurora has properties similar to a poleward moving auroral form (PMAF), which is regarded as the ionospheric signature of flux transfer event (FTE) or increased magnetopause reconnection (Fasel, 1995; Lockwood et al., 1993; Sandholt et al., 1986; Xing et al., 2012) that may propagate all the way across the polar cap (Nishimura et al., 2014).

Previous studies have shown that magnetopause reconnection can cause a series of ionospheric responses that can be identified by radars (Davis & Lockwood, 1997; Moen et al., 2008; Oksavik et al., 2004). Southwood (1987) put forward a model that predicts the field-aligned currents (FACs) and local ionospheric flow patterns due to a FTE. In order to better characterize the ionospheric signatures of throat aurora, we designed an experiment for the EISCAT Svalbard radar (ESR) in combination with all-sky cameras. The experiment enabled us for the first time to present a close phenomenological relationship between the ionospheric response and the throat aurora. The results are indispensable for a systematic understanding of throat aurora and the magnetosphere-ionosphere coupling in the dayside cusp region.

2. Experiment Design

The Yellow River Station (YRS; 78.9°N) at Ny-Alesund, Svalbard, is one of a few stations with a long time series of optical auroral observations on the dayside during the boreal winters in the northern hemisphere. Three all-sky cameras equipped with band-pass filters at 557.7, 630.0, and 427.8 nm, respectively, have been continuously operated since 2003 at YRS (Hu et al., 2009), and the throat aurora was first defined based on the auroral observations at YRS (Han et al., 2015).

The ESR is located at Longyearbyen, Svalbard, which is ~100 km south of YRS. The ESR has two antennas, a 32-m fully steerable parabolic dish antenna and a 42-m fixed parabolic antenna aligned along the direction of the local geomagnetic field. With the two antennas, ideally, we expect to detect the ionospheric flows around throat aurora with the 32-m radar by fast azimuth scans, and at the same time to monitor the ionospheric parameters at a fixed point around the poleward part of the throat aurora with the 42-m radar at higher time resolution. This idea is shown in Figure 1a. While designing the scan mode for the 32-m antenna, the key goal was to have the ESR beam intersect a throat aurora. From our past experience and knowledge, throat auroras often occur overhead YRS with an equatorward extension of ~2–3° in geomagnetic latitude. We therefore ran the 32-m antenna at a fixed elevation of 70°, with azimuth changing between 127° and 247° (which translates to ±60° centered on magnetic south for the ESR site) at a slow speed of 0.625 deg/s, as illustrated in Figure 1a. It is not common to operate the ESR in a scan mode at such a high-elevation angle due to the small field of view. However, it is highly desirable for our purpose, because we gain higher spatial resolution in the close vicinity of the throat aurora. Figure 1b illustrates the predictions of mesoscale FACs and ionospheric flow pattern due to a reconnection pulse at the magnetopause according to the model of Southwood (1987). Our experiment aims to test if the throat aurora shows similar characteristics to this model.

Observations were made from 27 to 30 November in 2017. On each day, the ESR ran from 07:00 to 12:00 UT, which is ~10:00–15:00 magnetic local time. Most of the experiment time was cloudy. However, on 27 November 2017, the sky became clear from 08:10 to 09:30 UT. Fortunately, typical throat auroras appeared during this short time interval that are exactly at the predicted location as illustrated in Figure 1a. This provided us with an unprecedented opportunity to characterize the ionospheric signatures of throat aurorae.

3. Coordinated Observations

Figure 2 shows a summary of the 32-m radar observation on 27 November 2017. From top to bottom, the panels show IMF B_x, B_y, and B_z components; solar wind density (N_p) and solar wind dynamic pressure (P_{dyn}); and the ESR basic plasma parameters of electron concentration (N_e), electron temperature (T_e), ion

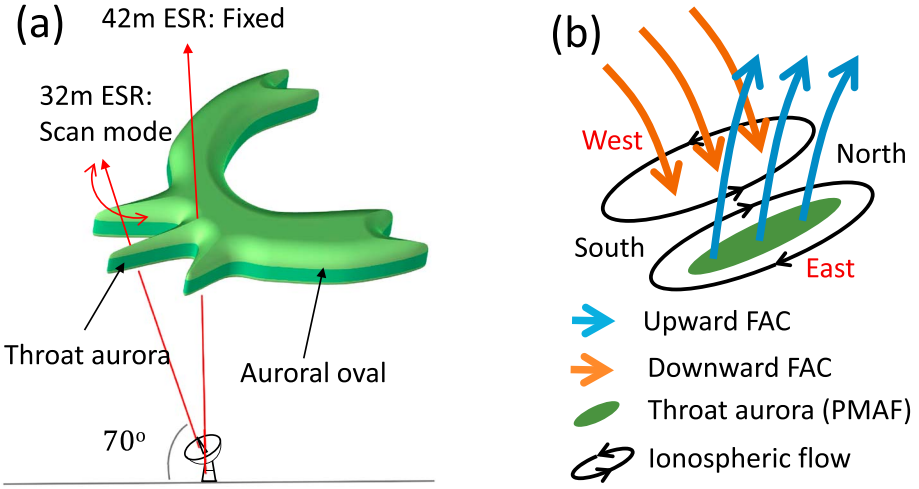

Figure 1. (a) Illustration of the observational geometry and experiment mode for EISCAT Svalbard Radar, with the steerable 32-m antenna at 70° elevation in a fast azimuth scan, and the fixed 42-m antenna pointing toward magnetic zenith. (b) Prediction of reconnection signatures in the ionosphere (currents, flow, and aurora) according to the Southwood (1987) model.

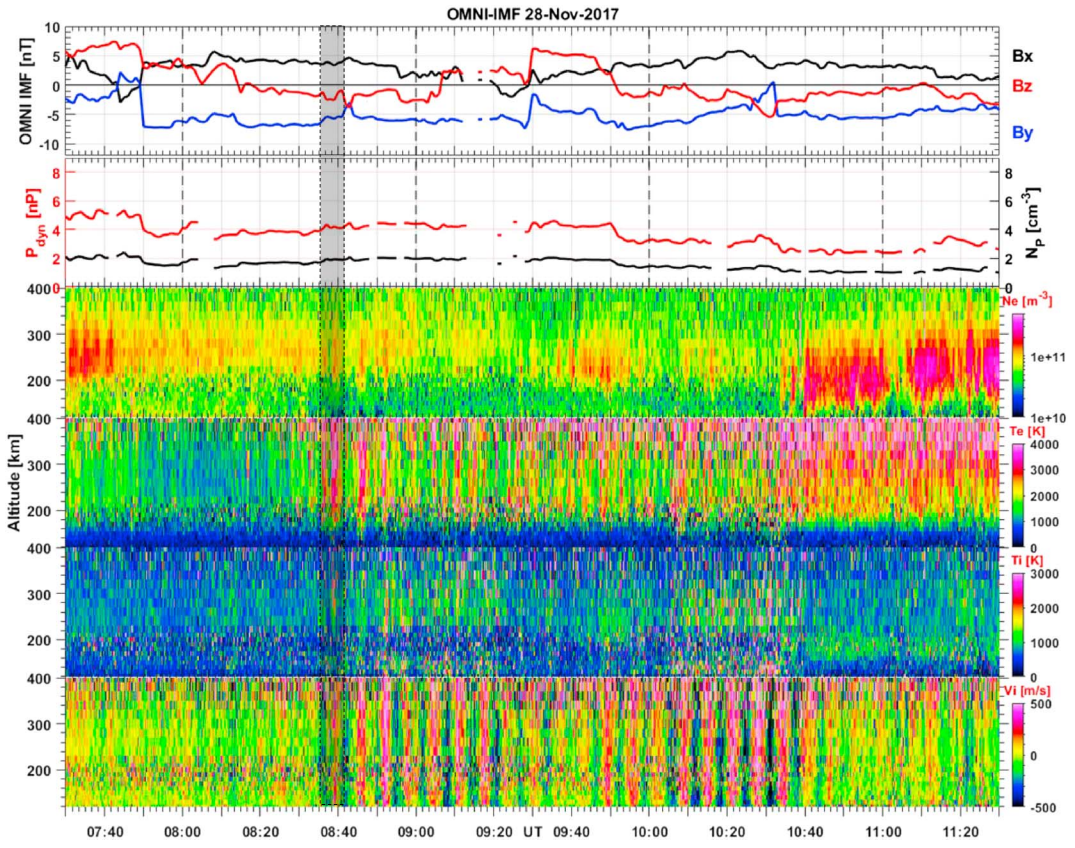

Figure 2. IMF conditions and a summary plot of the EISCAT Svalbard Radar 32-m antenna observations on 27 November 2017. The panels from top to bottom are IMF B_x, B_y, B_z; solar wind density (N_p) and solar wind dynamic pressure (P_{dyn}); and electron concentration (N_e), electron temperature (T_e), ion temperature (T_i), and line-of-sight velocity of ions (V_i), respectively. The shaded region indicates the time period when a detailed comparison between optical and radar observations is given.

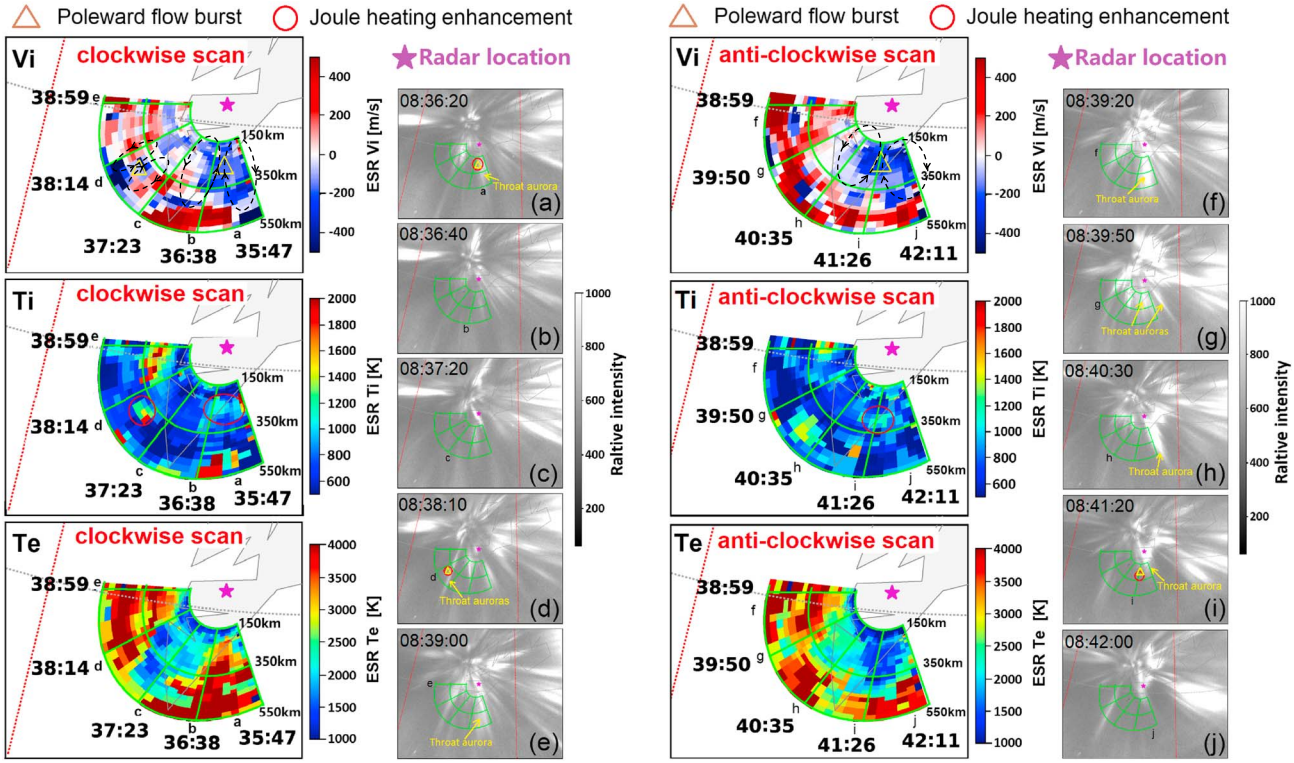

Figure 3. Two EISCAT Svalbard Radar 32-m antenna scans of V_i, T_i, and T_e from 08:35:47 to 08:42:11 UT on 27 December 2007 are compared to auroral observations. The radar and optical observations for the clockwise/counterclockwise scan are shown in the left/right two columns, respectively. The purple pentagons indicate the location of the ESR site. The fan-shaped grids show the coverage of the 32-m radar beam in the altitude range of 150–550 km. The letters "a"–"j" shown in bottom of the fan-shaped grid indicate the approximate directions of the radar beam at the time of the auroral images (a)–(j). The capture time of each auroral image is given in the top left corner on the image, and the throat auroras are indicated in yellow text. Yellow triangles inside the two V_i panels indicate antisunward flow bursts and are overlaid with the auroral images for easier comparison. Red circles in the T_i observations indicate some Joule heating events associated with the antisunward flow bursts, which are overlaid with the aurora images for easier comparison. In the V_i observations we infer mesoscale flow cells that are highlighted by black dashed circles with arrows.

temperature (T_i), and line-of-sight velocity of ions (V_i), respectively. The positive value of V_i means flow away from the radar for both the 32- and 42-m radars. In Figure 2, clear periodic variations, especially in V_i, were observed from 08:36 to 10:50 UT. The flow reversals observed at ~08:36–08:42 UT, as indicated by the shaded region, were coinciding in time with coordinated auroral observations, and a detailed comparison between optical and radar observations is shown in Figure 3.

Figure 3 shows the ESR 32-m radar observations of the V_i, T_i, and T_e during two successive scans from 08:35:47 to 08:42:11 UT together with simultaneous auroral images. The detailed description is given in the figure caption. As we can see in Figure 3, the auroras changed their shape very quickly during these scans. Under such conditions, it is the unique experimental design that enables us to make a detailed causal analysis between the optical and radar observations as follows:

1. Local flow pattern associated with throat aurora

In Figure 2, two short time periods of negative V_i were observed at ~08:36 and ~08:41 UT, as indicated by the two black arrows, which correspond to the labels “a” and “i” in Figure 3, respectively. Because the ESR was very close to magnetic noon, the negative V_i values around labels “a” and “i” reflect bursts of antisunward (poleward) flow. Compared with the auroral observation, these antisunward flow bursts were associated with the throat auroras as indicated in images (a) and (i), respectively. We should note that the throat aurora in image (i) first appeared in image (h). It moved poleward and became weak in image (i), which is a typical characteristic of PMAF.

A clear negative V_i value was also observed along beam “d” at ~400 km as marked by the yellow triangle. This corresponds to the *F* region and is associated with a throat aurora structure as indicated in image (d).

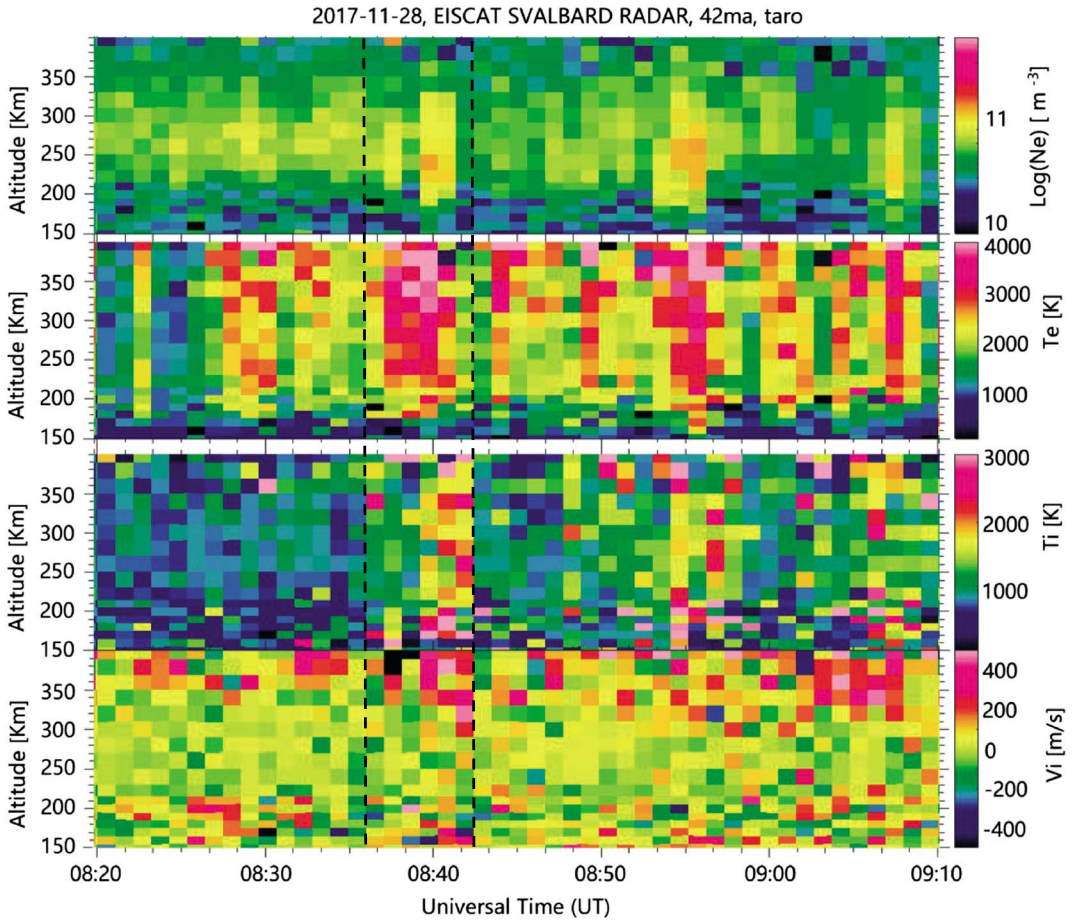

Figure 4. The N_e, T_e, T_i, and V_i observed by the EISCAT Svalbard Radar 42-m antenna, which is fixed and pointing toward the geomagnetic zenith. The two vertical dashed lines indicate the start and end time for the observations shown in Figure 3.

Besides the negative V_i values, we also observed a clear positive V_i at beam "c," which was located between the two negative V_i values of "a" and "d." We thus argue that these observations correspond to small-scale twin-vortex flow cells that are associated with the throat auroras, as indicated by the black dashed circles on the V_i observations in Figure 3.

2. Relative location between antisunward flow bursts and throat aurora

The observed T_i enhancements are caused by Joule heating (St.-Maurice & Hanson, 1982). For the V_i and T_i observations in Figure 3 we marked some antisunward flow bursts and T_i enhancements (Joule heating) by yellow triangles and red circles, respectively. These locations are overlaid on the auroral images. The antisunward flow bursts were almost coincident with the T_i enhancements (Joule heating), but were always observed at the western edge (toward dawn) of the corresponding throat auroras, indicating that the antisunward flow bursts give enhanced Joule heating along the western side of the throat auroras that are associated with an upward field-aligned current sheet. Furthermore, as indicated by the black dashed circles on Figure 3, we can see that the throat auroras (upward FACs) are located in the middle of the clockwise flow cells; while the middle of the counterclockwise flow cells correspond to downward FACs (absence of aurora). These findings are well consistent with the predicted geometry in the Southwood (1987) model (see Figure 1b).

3. Ion upflow associated with throat aurora

Figure 4 shows the N_e, T_e, T_i, and V_i observed by the ESR 42m, which is fixed toward geomagnetic zenith. The two vertical dashed lines indicate the start and end time of the scans shown in Figure 3. From ~08:39

to ~08:42 UT clear increases are observed in all these parameters. The high positive V_i values at high altitude here reflect ion upflow. Compared with the auroral observations in Figure 3, strong throat auroras were observed from 08:38:10 to 08:42:00 UT and the ESR 42m was directed at the poleward part of the throat auroras. The combined observations in Figures 3 and 4 suggest that the throat auroras were associated with ion upflows.

4. Discussion

The observational results above have the following implications:

1). Throat aurora being associated with magnetopause reconnection.

Throat aurora has been suggested to be caused by magnetopause reconnection (Han, 2019; Han et al., 2017), but observational evidence is not well established. FTEs near the magnetopause have been generally accepted as signatures of reconnection (Russell & Elphic, 1979). Southwood (1987) put forward a model to predict FTE signatures in the ionosphere, including (1) the fast moving newly opened flux, (2) an upward/downward pair of FACs on the flanks of the newly opened flux, and (3) the twin flow cells driven by the FACs. Some studies have searched for these signatures. For example, PMAFs (Fasel, 1995; Lockwood et al., 1993 ; Sandholt et al., 1986) and ionospheric flow bursts (e.g., Moen et al., 2008; Oksavik et al., 2004; Provan et al., 1998) have been suggested as signatures of FTEs. These studies were dominated by the IMF B_y and B_z components (i.e., B_x was small), but the current paper focuses on a different situation where IMF was dominated by the B_x and B_y components (i.e., B_z was small).

First, in Figure 3 the throat auroras in images (h) and (i) are the same feature, which moved poleward like a PMAF. In literature, PMAFs are interpreted as the ionospheric signatures of FTE (Lockwood et al., 1993; Sandholt et al., 1986). This can be regarded as the first evidence for throat aurora being associated with dayside magnetopause reconnection presented in this paper.

Second, as depicted in the V_i observations in Figure 3, we observed small-scale twin flow cells that were associated with the throat auroras. Such flow cells are similar in shape and size with the model prediction of Southwood (1987) of the ionospheric response due to a newly opened magnetic flux tube. In Figure 3 the antisunward flow bursts were co-located with the T_i enhancements, and were always observed west (dawnward) of the corresponding throat auroras. The Southwood (1987) model suggests that a pair of upward/dawnward FACs on the flanks of the newly opened flux tube drive the twin flow cells. The exterior flow serves to move the adjacent flux out of the way of the central tube as it moves. On the flanks, the flux actually moves antiparallel to the central flow and the central flow is antisunward. Because optical electron auroras are associated with the upward FACs, we can regard the throat aurora as one of the flanks of the newly opened flux tube. The antisunward flow bursts can be regarded as the central flow. We can also infer that the middle of the counterclockwise flow cells should be coincident with the downward FACs. Thus, we argue that the displacements between throat aurora and flow bursts observed in this paper are consistent with the Southwood (1987) model as illustrated in Figure 1b and thus directly links throat aurora to expected reconnection signatures.

We should make one important note. In previous studies of PMAFs and FTE signatures (e.g., Moen et al., 2008; Oksavik et al., 2004) for small B_x (large B_y and B_z) the flow channels were elongated in the magnetic east-west direction and parallel to the aurora oval. In our work, for small B_z (and large B_y and B_x), the throat aurora flow bursts were aligned in the magnetic north-south direction and perpendicular to the aurora oval.

Davis and Lockwood (1997) predicted that, for a field-aligned operation of the ESR, reconnection pulses will be seen as enhancements in the electron concentration and temperature. Moen et al. (2004) and Skjaeveland et al. (2011) showed that the PMAFs were associated with enhancements of T_e and T_i. In Figure 4, the observations from ~08:39 to ~08:42 UT show that clear enhancements of T_e and T_i were observed associated with a throat aurora. This provides further evidence for the throat aurora being associated with reconnection.

2). Agreement with a conceptual model of throat aurora

Observations show that the occurrence of throat aurora depends on factors either inside or outside the magnetosphere (Han et al., 2017). In order to explain these observational results, Han (2019) proposed a conceptual model of throat aurora, which suggests that an ionospheric polarization electric field in the dusk-to-

dawn (east-to-west) direction plays a key role for the generation of throat aurora. Using a full particle simulation, Tu et al. (2008) suggested that the usual $E \times B$ motion for single particle does not apply when the mutual interaction (Coulomb force) between the ion and electron is considered. If an external electric field is applied to a magnetized plasma, the ions and electrons will be separated to build a plasma sheath that tends to shield the externally applied electric field (Tu et al., 2008). If the dusk-to-dawn electric field does exist during the generation process of throat aurora, as proposed by Han (2019), the ions and electrons involved will be spatially separated, with electrons to the east and ions to the west. It leads to the upward and downward FACs that are always located east and west of the newly opened flux tube, just as observed in the current paper. The relative location of the upward and downward FACs therefore supports the Han (2019) model and is an important observational property of throat aurora.

3). First observation of the ionospheric responses of throat aurora

Although it has been confirmed that throat auroras correspond to magnetopause indentations (Han et al., 2016, 2018) and have high occurrence rate (Han et al., 2017), many observational details of throat auroras are still unclear.

Joule heating is one of the three important energy inputs into the Earth's ionosphere, along with extreme ultraviolet radiation and particle precipitation (McHarg et al., 2005). The local Joule heating rate is essentially decided by the intrinsic electric field. For the throat auroras, the small-scale flow cells as indicated in Figure 3 were suggested to be associated with small-scale electric fields in the ionosphere (Southwood, 1987). The contributions to Joule heating of small-scale electric field in the ionosphere can be more than a factor of 2 greater than the mean field contribution regardless of geomagnetic conditions, and at times even larger (Hurd & Larsen, 2016). Therefore, we believe that the local Joule heating effects in Figures 3 and 4 were linked to small-scale electric fields, which demonstrates that throat auroras could play an important role for thermospheric heating in the cusp (Lühr et al., 2004).

We also observed clear ion upflow associated with the throat aurora in Figure 4. The Joule heating and soft particle precipitation have been suggested as energy sources driving both ion upflow and neutral upwelling in the topside ionosphere (Lühr et al., 2004; Moen et al., 2004; Ogawa et al., 2003; Skjaeveland et al., 2011; Strangeway et al., 2005; Yau et al., 1985). Ogawa et al. (2003) found that soft particle precipitation triggers ion upflow in the open field line regions of the high-latitude dayside ionosphere. Moen et al. (2004) found one-to-one correspondences between upflows and PMAFs. Throat auroras are caused by soft particle precipitation from the magnetosheath (Han et al., 2016) and display properties similar to PMAF (Chen et al., 2017). So it is not surprising to observe ion upflows associated with throat aurora as shown in Figure 4.

The current study focuses on revealing the observational characteristics of the ionospheric response associated with throat aurora, so we will not discuss the generation mechanisms any further. However, these observational results are themselves indispensable for a systematic understanding of throat aurora.

5. Conclusions

A unique experiment for the ESR for the first time documented a close phenomenological relationship between ionospheric variations and throat aurora. These results provide clear evidence that throat aurora is associated with expected signatures of magnetopause reconnection events. In addition, our results are consistent with the throat aurora model of Han (2019). These results are indispensable for fully understanding the generation processes of magnetopause indentations and their resultant ionospheric responses.

Acknowledgments
This work was supported by the National Natural Science Foundation of China (41831072, 41774174, 41704159, 41431072) and National Key R&D Program of China (2018YFC1407303). K.O. acknowledges financial support from the Norwegian Research Council under the contract 223252. EISCAT is an international association supported by research organizations in China (CRIRP), Finland (SA), Japan (NIPR and ISEE), Norway (NFR), Sweden (VR), and the United Kingdom (UKRI). Our ESR experiment was supported by National Key Laboratory of Electromagnetic Environment, China Research Institute of Radiowave Propagation, Qingdao, China. Auroral observations at YRS are supported by CHINARE and provided by PRIC through http://www.chinare.org.cn/aurora/dataquery.

References

Chen, X. C., Han, D. S., Lorentzen, D. A., Oksavik, K., Moen, J. I., & Baddeley, L. J. (2017). Dynamic properties of throat aurora revealed by simultaneous ground and satellite observations. *Journal of Geophysical Research: Space Physics*, *122*, 3469–3486. https://doi.org/10.1002/2016JA023033

Davis, C. J., & Lockwood, M. (1997). Predicted signatures of pulse reconnection in ESR data. *Annales Geophysicae*, *14*(12), 1246–1256.

Fasel, G. J. (1995). Dayside poleward moving auroral forms: A statistical study. *Journal of Geophysical Research*, *100*(A7), 11,891–11,905. https://doi.org/10.1029/95JA00854

Han, D., Chen, X.-C., Liu, J.-J., Qiu, Q., Keika, K., Hu, Z.-J., et al. (2015). An extensive survey of dayside diffuse aurora based on optical observations at Yellow River Station. *Journal of Geophysical Research: Space Physics*, *120*, 7447–7465. https://doi.org/10.1002/2015ja021699

Han, D. S., Hietala, H., Chen, X. C., Nishimura, Y., Lyons, L. R., Liu, J. J., et al. (2017). Observational properties of dayside throat aurora and implications on the possible generation mechanisms. *Journal of Geophysical Research: Space Physics*, *122*, 1853–1870. https://doi.org/10.1002/2016ja023394

Han, D.-S., Liu, J. J., Chen, X. C., Xu, T., Li, B., Hu, Z. J., et al. (2018). Direct evidence for throat aurora being the ionospheric signature of magnetopause transient and reflecting localized magnetopause indentations. *Journal of Geophysical Research: Space Physics*, *123*, 2658–2667. https://doi.org/10.1002/2017ja024945

Han, D.-S., Nishimura, Y., Lyons, L. R., Hu, H. Q., & Yang, H. G. (2016). Throat aurora: The ionospheric signature of magnetosheath particles penetrating into the magnetosphere. *Geophysical Research Letters*, *43*, 1819–1827. https://doi.org/10.1002/2016gl068181

Han, D. (2019). Ionospheric polarization electric field guiding magnetopause reconnection: A conceptual model of throat aurora. *Science China Earth Sciences*, *62*. https://doi.org/10.1007/s11430-019-9358-8

Hao, Y., Lembege, B., Lu, Q., & Guo, F. (2016). Formation of downstream high-speed jets by a rippled nonstationary quasi-parallel shock: 2-D hybrid simulations. *Journal of Geophysical Research: Space Physics*, *121*, 2080–2094. https://doi.org/10.1002/2015ja021419

Hu, Z. J., Yang, H., Huang, D., Araki, T., Sato, N., Taguchi, M., et al. (2009). Synoptic distribution of dayside aurora: Multiple-wavelength all-sky observation at Yellow River Station in Ny-Ålesund, Svalbard. *Journal of Atmospheric and Solar-Terrestrial Physics*, *71*(8-9), 794–804. https://doi.org/10.1016/j.jastp.2009.02.010

Hurd, L. D., & Larsen, M. F. (2016). Small-scale fluctuations in barium drifts at high latitudes and associated Joule heating effects. *Journal of Geophysical Research: Space Physics*, *121*, 779–789. https://doi.org/10.1002/2015ja021868

Lockwood, M., Denig, W. F., Farmer, A. D., Davda, V. N., Cowley, S. W. H., & Lühr, H. (1993). Ionospheric signatures of pulsed reconnection at the Earth's magnetopause. *Nature*, *361*(6411), 424–428. https://doi.org/10.1038/361424a0

Lühr, H., Rother, M., Köhler, W., Ritter, P., & Grunwaldt, L. (2004). Thermospheric up-welling in the cusp region: Evidence from CHAMP observations. *Geophysical Research Letters*, *31*, L06805. https://doi.org/10.1029/2003GL019314

McHarg, M., Chun, F., Knipp, D., Lu, G., Emery, B., & Ridley, A. (2005). High-latitude Joule heating response to IMF inputs. *Journal of Geophysical Research*, *110*, A08309. https://doi.org/10.1029/2004JA010949

Moen, J., Oksavik, K., & Carlson, H. C. (2004). On the relationship between ion upflow events and cusp auroral transients. *Geophysical Research Letters*, *31*, L11808. https://doi.org/10.1029/2004GL020129

Moen, J., Rinne, Y., Carlson, H. C., Oksavik, K., Fujii, R., & Opgenoorth, H. (2008). On the relationship between thin Birkeland current arcs and reversed flow channels in the winter cusp/cleft ionosphere. *Journal of Geophysical Research*, *113*, A09220. https://doi.org/10.1029/2008JA013061

Nishimura, Y., Lyons, L. R., Zou, Y., Oksavik, K., Moen, J. I., Clausen, L. B., et al. (2014). Day-night coupling by a localized flow channel visualized by polar cap patch propagation. *Geophysical Research Letters*, *41*, 3701–3709. https://doi.org/10.1002/2014GL060301

Ogawa, Y., Fujii, R., Buchert, S. C., Nozawa, S., & Ohtani, S. (2003). Simultaneous EISCAT Svalbard radar and DMSP observations of ion upflow in the dayside polar ionosphere. *Journal of Geophysical Research*, *108*(A3), 1101. https://doi.org/10.1029/2002JA009590

Oksavik, K., Moen, J., & Carlson, H. C. (2004). High-resolution observations of the small-scale flow pattern associated with a poleward moving auroral form in the cusp. *Geophysical Research Letters*, *31*, L11807. https://doi.org/10.1029/2004GL019838

Plaschke, F., Hietala, H., Archer, M., Blanco-Cano, X., Kajdič, P., Karlsson, T., et al. (2018). Jets downstream of collisionless shocks. *Space Science Reviews*, *214*(5), 81. https://doi.org/10.1007/s11214-018-0516-3

Provan, G., Yeoman, T. K., & Milan, S. E. (1998). CUTLASS Finland radar observations of the ionospheric signatures of flux transfer events and the resulting plasma flows. *Annales Geophysicae*, *16*(11), 1411–1422. https://doi.org/10.1007/s00585-998-1411-0

Rodriguez, J. V., Carlson, H. C., & Heelis, R. A. (2012). Auroral forms that extend equatorward from the persistent midday aurora during geomagnetically quiet periods. *Journal of Atmospheric and Solar-Terrestrial Physics*, *86*, 6–24. https://doi.org/10.1016/j.jastp.2012.06.001

Russell, C. T., & Elphic, R. C. (1979). ISEE observations of flux transfer events at the dayside magnetopause. *Geophysical Research Letters*, *6*(1), 33–36. https://doi.org/10.1029/GL006i001p00033

Sandholt, P. E., Deehr, C. S., Egeland, A., Lybekk, B., Viereck, R., & Romick, G. J. (1986). Signatures in the dayside aurora of plasma transfer from the magnetosheath. *Journal of Geophysical Research*, *91*(A9), 10,063–10,079. https://doi.org/10.1029/JA091iA09p10063

Skjaeveland, Å., Moen, J., & Carlson, H. C. (2011). On the relationship between flux transfer events, temperature enhancements, and ion upflow events in the cusp ionosphere. *Journal of Geophysical Research*, *116*, A10305. https://doi.org/10.1029/2011ja016480

Southwood, D. J. (1987). The ionospheric signature of flux transfer events. *Journal of Geophysical Research*, *92*(A4), 3207. https://doi.org/10.1029/JA092iA04p03207

St.-Maurice, J. P., & Hanson, W. B. (1982). Ion frictional heating at high latitudes and its possible use for an in situ determination of neutral thermospheric winds and temperatures. *Journal of Geophysical Research*, *87*(A9), 7580. https://doi.org/10.1029/JA087iA09p07580

Strangeway, R. J., Ergun, R. E., Su, Y.-J., Carlson, C. W., & Elphic, R. C. (2005). Factors controlling ionospheric outflows as observed at intermediate altitudes. *Journal of Geophysical Research*, *110*, A03221. https://doi.org/10.1029/2004JA010829

Tu, J., Song, P., Reinisch, B. W., Song, P., Foster, J., Mendillo, M., & Bilitza, D. (2008). On the concept of penetration electric field. In *AIP Conference Proceedings* (*974*, pp. 81–85).

Xing, Z. Y., Yang, H. G., Han, D. S., Wu, Z. S., Hu, Z. J., Zhang, Q. H., et al. (2012). Poleward moving auroral forms (PMAFs) observed at the Yellow River Station: A statistical study of its dependence on the solar wind conditions. *Journal of Atmospheric and Solar-Terrestrial Physics*, *86*, 25–33. https://doi.org/10.1016/j.jastp.2012.06.004

Yau, A. W., Lenchyshyn, L., Shelley, E. G., & Peterson, W. K. (1985). Energetic auroral and polar ion outflow at DE 1 altitudes: Magnitude, composition, magnetic activity dependence, and long-term variations. *Journal of Geophysical Research*, *90*(A9), 8417–8432. https://doi.org/10.1029/JA090iA09p08417